


---

This is the **accepted version** of the journal article:

Knipping, Etienne; Aucher, C.; Guirado López, Gonzalo; [et al.]. «Room temperature ionic liquids versus organic solvents as lithium-oxygen battery electrolytes». New journal of chemistry, Vol. 42, Issue 6 (March 2018), p. 4693-4699. DOI 10.1039/c8nj00449h

---

This version is available at <https://ddd.uab.cat/record/274572>

under the terms of the  **IN**  
COPYRIGHT license

# Room Temperature Ionic Liquids versus organic solvents as lithium-oxygen battery electrolytes

E. Knipping,<sup>a,b</sup> C. Aucher,<sup>a</sup> G. Guirado<sup>b</sup> and L. Aubouy<sup>a</sup>

<sup>a</sup> *Leitat Technological Center, Carrer de la Innovació, 2 08225 Terrassa, Spain.*

<sup>b</sup> *Departament de Química, Universitat Autònoma de Barcelona, E-08193 Bellaterra, Barcelona, Spain.*

\*E-mail: [eknipping@leitat.org](mailto:eknipping@leitat.org)

Imidazolium, pyrrolidinium and piperidinium room temperature ionic liquids (RTILs) are characterized to evaluate their thermal stability, ionic conductivity, viscosity, potential window and lithium solvation, which are key parameters for lithium-oxygen (Li-O<sub>2</sub>) battery electrolytes. The electrochemical tests of these RTILs are also carried out in Li-O<sub>2</sub> cells and show reasonable values of specific capacity, up to 1659 mAh per gram of carbon in case of 1-propyl-3-methylimidazolium bis(trifluoromethylsulfonyl)imide (PMI TFSI) with 0.2 molar fraction of LiTFSI. RTILs are compared with conventional organic electrolytes like ethylene carbonate (EC)/diethyl carbonate (DEC) solution or the tetraethylene glycol dimethyl ether (TEGDME), which enables to provide a further insight into ways of improving the electrolyte properties for Li-O<sub>2</sub> battery. In particular, a viscosity lower than 100 cP combined with a lithium coordination number lower than 1.5 tends to enhance the battery performance.

Key words: room temperature ionic liquid, electrolyte, Li-O<sub>2</sub> battery, ionic conductivity, lithium solvation.

## Introduction

The Li-O<sub>2</sub> battery has received much interest in the last few years as global energy demand is growing and availability of fossil energies becomes limited. At present, Li-ion batteries are limited to 250-300 Wh kg<sup>-1</sup> at the cell level whereas the new approach of Li-O<sub>2</sub> batteries offers a theoretical specific energy superior to 1000 Wh kg<sup>-1</sup>.<sup>1-5</sup> This value is comparable to the actual internal combustion engine technology (ICE). Moreover, the population growth and the European policy that targets to reduce the CO<sub>2</sub> emissions by 40% by 2030<sup>6</sup> push to the transportation electrification. From this context and regarding the potential of this new technology, the main application for Li-O<sub>2</sub> battery is electric vehicles (EV), with the possibility in the next few years to develop an electric car with same distance range as gasoline powered car but cheaper and more environmentally friendly. However, this new technology will remain a research topic for at least the next 20 following years, due to the low cyclability, the limited electrical efficiency, the low rate capability and the difficulty of assembling a safe practical cell working in ambient atmosphere better than at the laboratory scale under well-controlled conditions. Indeed, since the battery reaction is not fully reversible, the capacity drastically decreases after 20 cycles in most cases.<sup>7</sup> The main cause of this irreversibility is the formation of Li<sub>x</sub>O<sub>y</sub> (x, y = 1, 2) discharge products, since they are insoluble in the electrolyte and lead to the degradation of the battery components.<sup>8</sup> In particular, the cathode's pores hosting the reaction between the lithium ions and the oxygen become obstructed<sup>3</sup> and besides, the anodic lithium, which is a very reactive metal, forms a hydroxide layer preventing the diffusion of lithium ions.<sup>7</sup>

One of the biggest challenge to progress in Li-O<sub>2</sub> batteries is the development of an electrolyte that requires the following characteristics: (i) compatibility with the anode, (ii) low volatility to avoid the evaporation of the solvent in open cell systems, (iii) high oxygen solubility and diffusivity, (iv) a low viscosity to ensure fast kinetics of mass transport and a high ionic conductivity and (v) a wide electrochemical stability window.<sup>9</sup> Usual carbonate solvents, such as ethylene carbonate (EC), propylene carbonate (PC) and diethyl carbonate (DEC) from the lithium-ion technology would be good candidates with their stability at high potentials, their ability to form a stable solid electrolyte interphase (SEI) on lithium and their high polarity that enables to transport lithium cations effectively. The main drawback associated with those solvents is their reactivity towards a nucleophilic attack of the superoxide (O<sub>2</sub><sup>-</sup>) coming from the ORR.<sup>10,11</sup> Then the decomposition of the carbonate, forming mostly lithium carbonate will result to the passivation of the cathode and a very poor cycle life of the battery.<sup>10,12</sup> On the other hand, ether solvents are more stable to the superoxide and the discharge products and show the advantages of cathodic stability and low volatility.<sup>13</sup> Both 1,2-dimethoxyethane (DME) and tetraethylene glycol dimethyl ether (TEGDME) are the most-used ether solvents as they form the most of Li<sub>2</sub>O<sub>2</sub> during discharge and evolved the most

oxygen during charge.<sup>14</sup> However, the degradation of these electrolytes has been observed with the formation of side products like acetates, formates and carbonates,<sup>10</sup> which makes them unsuitable for a practical commercial battery.

Recently, Room Temperature Ionic Liquids (RTILs) attracted much attention. 1,3-dialkylimidazolium bis(trifluoromethylsulfonyl)imide ionic liquids are known for their thermal and electrochemical stability and high conductivity.<sup>15</sup> Ammonium and phosphonium cations with long alkyl chain showed large cathodic potential window and high oxygen solubility.<sup>16</sup> Pyrrolidinium ionic liquids exhibited a reasonable ionic conductivity ( $> 1 \text{ mS cm}^{-1}$ ) and a cathodic stability limit exceeding the lithium plating/stripping potential.<sup>17</sup> Hence, the high thermal stability, non-flammability, low vapour pressure and wide potential window of RTILs can offer an interesting alternative to the traditional organic solvents for Li-O<sub>2</sub> battery electrolyte.<sup>12,18–22</sup> Nakamoto et al.<sup>11</sup> showed the advantage of the RTILs stability against electrochemical oxidation vs. Li<sup>+</sup>/Li and O<sub>2</sub> redox reversibility. Cai et al.<sup>23</sup> proved that ionic liquid could show higher specific capacity compared to carbonate solvent electrolyte and Cechetto et al.<sup>24</sup> observed a decrease of 0.4 V of the overpotential by mixing ionic liquids with an ether-based electrolyte.

In this paper, we report on the study of the properties of several organic and ionic liquid-based electrolytes and their performance in Li-O<sub>2</sub> battery cells. The main chemical and physical properties of 9 different electrolytes are characterized before testing them in Li-O<sub>2</sub> battery cell in order to compare their electrochemical performance with respect to the electrolyte intrinsic properties. Both glyme and carbonate-based organic solvents used in lithium batteries are also studied and compared with the most performing RTILs for the Li-O<sub>2</sub> battery technology.

## Experimental

### Sample preparation

All ionic liquids, 99% pure, were purchased from IoLiTec (Ionic Liquids Technologies GmbH). The molecular structure of the RTIL ions studied is shown in the Figure 1. TEGDME, EC and DEC were purchased from Sigma Aldrich with purity higher than 99% as well as the salts of lithium bis(trifluoromethanesulfonyl)imide (LiTFSI – 99.95%) and lithium hexafluorophosphate (LiPF<sub>6</sub> – 99.99%). Nine electrolytes are prepared by direct mixing of appropriate amount of salt with either a RTIL or a solvent to reach the molar fraction of  $x = 0.2$ . The water content of all samples is measured by Karl Fischer (Coulometer KF 831) titration, before and after drying the electrolyte with 4 Å molecular sieves (Aldrich) for two days and stored in argon filled glove box (H<sub>2</sub>O < 1 ppm, O<sub>2</sub> < 1 ppm). To exclude the influence of water contamination in the electrolyte, which could affect its stability and the cyclability of the battery,<sup>23</sup> the water content of the ionic liquids is lowered until it reaches values between 43 and 322 ppm (Table 1). The same range as for the organic solvents is then obtained.

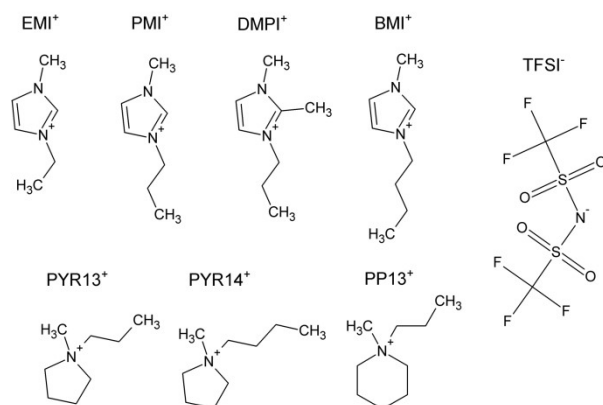


Figure 1. Molecular structure of the RTIL ions used. EMI: 1-Ethyl-3-methylimidazolium; PMI: 1-Methyl-3-propylimidazolium; DMPI: 1,2-Dimethyl-3-propylimidazolium; BMI: 1-Butyl-3-methylimidazolium; PYR13: 1-Methyl-1-propylpyrrolidinium; PYR14: 1-Butyl-1-methylpyrrolidinium; PP13: 1-Methyl-1-propylpiperidinium; TFSI: bis(trifluoromethylsulfonyl)imide.

### Ionic conductivity, viscosity, thermal stability

The ionic conductivity is measured with a titanium tip (Ref. 50 73) on an EC Meter Basic 30+ conductimeter (Crisson Instrument) in a range of temperature from -10 °C to 80 °C. The viscosities are measured using a Malvern Bohlin CVO 100-901 rheometer in air, at room temperature. Shear rates are varied between 0.1 s<sup>-1</sup> and 10 s<sup>-1</sup>. No shear thinning behavior due to the variation of the shear rate is observed. Hence, the viscosities are determined from the plateau value at all shear rates. Thermo gravimetric analysis is done with a TA Instrument Q500 apparatus, applying a ramp of 10 °C min<sup>-1</sup> until 800 °C in O<sub>2</sub> and N<sub>2</sub> atmosphere.

### Raman spectroscopy

The Raman spectra are recorded using a Bruker RFS/100 FT-Raman spectrometer with a Nd-YAG laser (wavelength of 1064 nm). The collected spectra are the average of 512 scans at an optical resolution of 2 cm<sup>-1</sup>. The samples are sealed in glass ampoules under argon and measured at room temperature. For a detailed analysis of the region 730-770 cm<sup>-1</sup>, the RTILs spectra are fit with the multipeak fitting package in IGOR PRO 6.37 using a Voigt function with a fixed Lorentzian/Gaussian ratio, following the procedure of Lassègues *et al.*<sup>25</sup> The lithium coordination numbers are calculated for each RTIL electrolyte from the deconvoluted spectra, dividing the area of the band corresponding to Li<sup>+</sup> coordinated anions with the total band area (including also the contributions from “free” anion) and the molar fraction of Li salt x.

### Electrochemical characterization

The electrochemical stability window of the electrolytes is determined with linear sweep voltammetry measured on a 3 mm-diameter platinum working electrode with lithium metal counter and reference electrodes at a scanning rate of 1 mV s<sup>-1</sup>. The potential is scanned from the open circuit voltage toward positive and negative potentials to evaluate the anodic and cathodic limit respectively.

Li-O<sub>2</sub> batteries are assembled inside an Ar-filled glove box using ECC-air cell (EL-Cell). The cathode for the Li-O<sub>2</sub> battery is prepared from a mixture of 90wt% PICA<sup>®</sup> (PICA) and 10wt% polyvinylidene fluoride (PVdF Kynar ADX 161, Arkema) in N-methyl-2-pyrrolidone (NMP, 99.5%, Sigma-Aldrich). The PICA<sup>®</sup> is an activated carbon with a mesoporous volume of 0.68 cm<sup>3</sup> g<sup>-1</sup>, suitable for Li-O<sub>2</sub> battery cathode.<sup>8</sup> A full description of this material is given by Brousse *et al.*<sup>26</sup> The slurry is tape casted on a Gas Diffusion Layer (GDL SIGRACET 24BC – SGL Company) using the doctor blade technique up to an active loading of 1.5 mg cm<sup>-2</sup>. Although this GDL may participate to the overall capacity of the battery,<sup>27</sup> only the mass of PICA is taken into account to normalize the specific capacity calculated. A circular lithium chip (Ref: EQ-Lib-LiC25, MTI Corp.) is used as the anode. The separator is a glass fiber membrane (Whatman GF/A) soaked with the tested electrolyte. The thick 260 µm is ensuring that the electrolyte is in excess with at least 100 µL. Prior applying any current, the cell is maintained under O<sub>2</sub> flow (8 mL min<sup>-1</sup>) up to stabilize the open circuit voltage after 10 hours. Galvanostatic tests are performed using a VMP3 Biologic instrument with a current of 100 µA cm<sup>-2</sup> applied between 2.15 V and 4.35 V with an oxygen flow rate of 8 mL min<sup>-1</sup> for the full initial discharge measurement. For the cycling test, discharge and recharge curves are recorded at a constant specific current of 75 µA cm<sup>-2</sup> within limited capacity of 500 mAh g<sup>-1</sup>.

## Results and discussion

The properties of the 9 studied electrolytes, including 7 RTILs and 2 organic solvents, are gathered in the Table 1. All the RTIL electrolyte formulations contain the same anion (TFSI) and a 0.2 molar fraction of LiTFSI. The use of TFSI guarantees the hydrophobic character of the electrolyte as well as a good electrochemical performance. The use of different anions would allow tuning the physico-chemical properties of the solvent, such as viscosity or conductivity. Two of the most common organic electrolyte formulations are also studied for comparison.

### Thermal stability

TGA experiments show two different trends in function of the electrolyte composition (Figure 2). For organic electrolytes, such as EC:DEC (2:1)-LiPF<sub>6</sub> and TEGDME-LiTFSI, a weight loss is observed either as soon as the measurement begins in the case of EC/DEC-LiPF<sub>6</sub> or at about 150°C in the case of TEGDME-LiTFSI, which corresponds to the EC/DEC or TEGDME evaporation.<sup>28–30</sup> However, when RTILs are used as an electrolytes the degradation temperature, with or without salt, is considerably higher (between 350 and 450°C). Hence, those TGA profiles indicate that RTILs can be safely used in a wider range of temperature than the organic electrolytes, which may enable to increase the safety of current batteries using organic solvent.<sup>31</sup> This would be one of the major advantages of ionic liquids as battery electrolytes.

The influence of oxygen in the thermal stability of the electrolytes is also evaluated in order to be in conditions as similar as possible to the operating conditions of Li-O<sub>2</sub> technology. In presence of oxygen the degradation temperature is obtained up to 20 °C lower with respect to the same test run under nitrogen atmosphere (Table 1). Indeed, degradation reactions occur at lower temperature in a more oxidizing environment, which is why the actual temperature range of ionic liquid stability is lower than the one measured under inert condition by TGA.<sup>32</sup> However, this slight decrease is not an issue considering the important gap between both RTILs and organic solvents thermal stability.

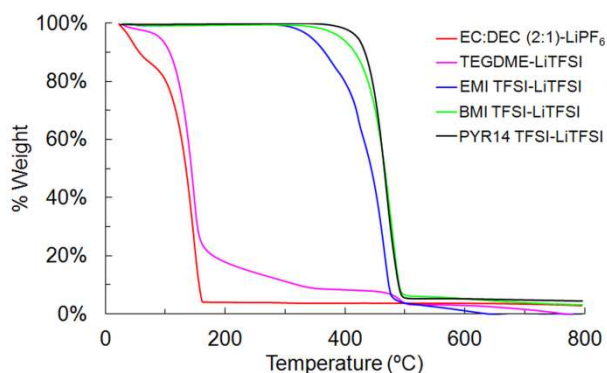


Figure 2. TGA spectra of ionic liquids and organic electrolytes measured under nitrogen atmosphere.

### Ionic conductivity

A higher ionic conductivity of the electrolyte enables to reduce the resistance of the system, to lower the overpotential and then to improve the reversibility of the system for higher current density applied.<sup>33</sup> The dependence of the ionic conductivity of different electrolytes with the temperature is shown in Figure 3. Again two different behaviors are observed, for organic electrolytes the conductivity with the temperature reveals that the TEGDME-LiTFSI reaches a maximum conductivity of 1.9 mS cm<sup>-1</sup> from 25 to at least 70 °C, whereas the ionic liquids have an increasing conductivity with the temperature.

Focusing on ionic liquids electrolytes, it clearly appears that the EMI TFSI-LiTFSI has the best ionic conductivity (from 3 to 7.5 mS cm<sup>-1</sup> at temperature between 0 and 80 °C). Then, BMI TFSI-LiTFSI and PYR14 TFSI-LiTFSI are in the same range as the TEGDME-LiTFSI with an ionic conductivity between 1 and 4 mS cm<sup>-1</sup>. These results can be easily rationalized taking into account the viscosity of the different RTILs electrolytes depicted in Table 1. A low viscosity value of the RTIL solvent, which in fact is related with a larger asymmetry in the cation structure, helps the mobility of the charge carriers<sup>34</sup> leading to a higher conductivity value of the electrolyte. Finally, it is worthy to note that the electrolytes based on organic solvent follow the same general trend.

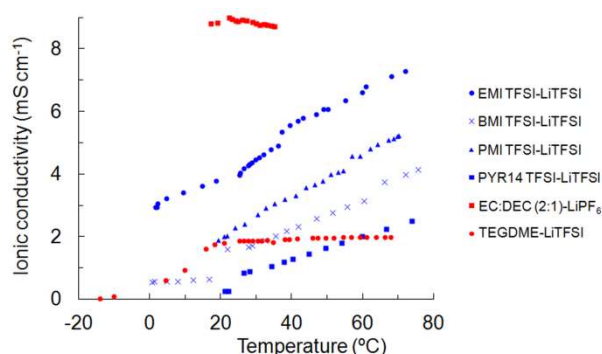


Figure 3. Ionic conductivity versus temperature for different families of electrolytes: in blue the RTILs and in red the organic solvents.

## Lithium coordination

The ion-ion interactions taking place in the electrolytes studied are investigated using Raman spectroscopy. As reported by several authors,<sup>25,35–37</sup> in TFSI-based RTILs the coordination of the anion [TFSI]<sup>−</sup> can be evaluated considering the peak at a wavenumber of  $\approx 742\text{ cm}^{-1}$ . Such a peak is associated to the anion expansion and contraction. In the presence of Li<sup>+</sup> cations, the TFSI<sup>−</sup> anions coordinating with Li<sup>+</sup> generate an additional signal, which is shifted to higher wavenumbers in the Raman spectra (Figure 4). As shown, the areas  $A_{\text{coordinating}}$  of this peak and  $A_{\text{non-coord}}$  of the non-coordinating TFSI<sup>−</sup> peak are strongly dependent on the cation-anion interaction occurring in the RTIL. The comparison of both areas is used to determine the lithium coordination number of the electrolyte (Table 1, Figure 4). The stronger is the anion-cation interaction occurring in the RTIL, the lower is the lithium coordination number. Thus the values obtained increase in the following order PMI TFSI-LiTFSI < PYR13 TFSI-LiTFSI < BMI TFSI-LiTFSI < EMI TFSI-LiTFSI < PYR14 TFSI-LiTFSI < DMPI TFSI-LiTFSI < PP13 TFSI-LiTFSI. These results show that the cation chemistry such as the number of protons and the ring size has a strong influence on the lithium coordination number.<sup>35</sup>

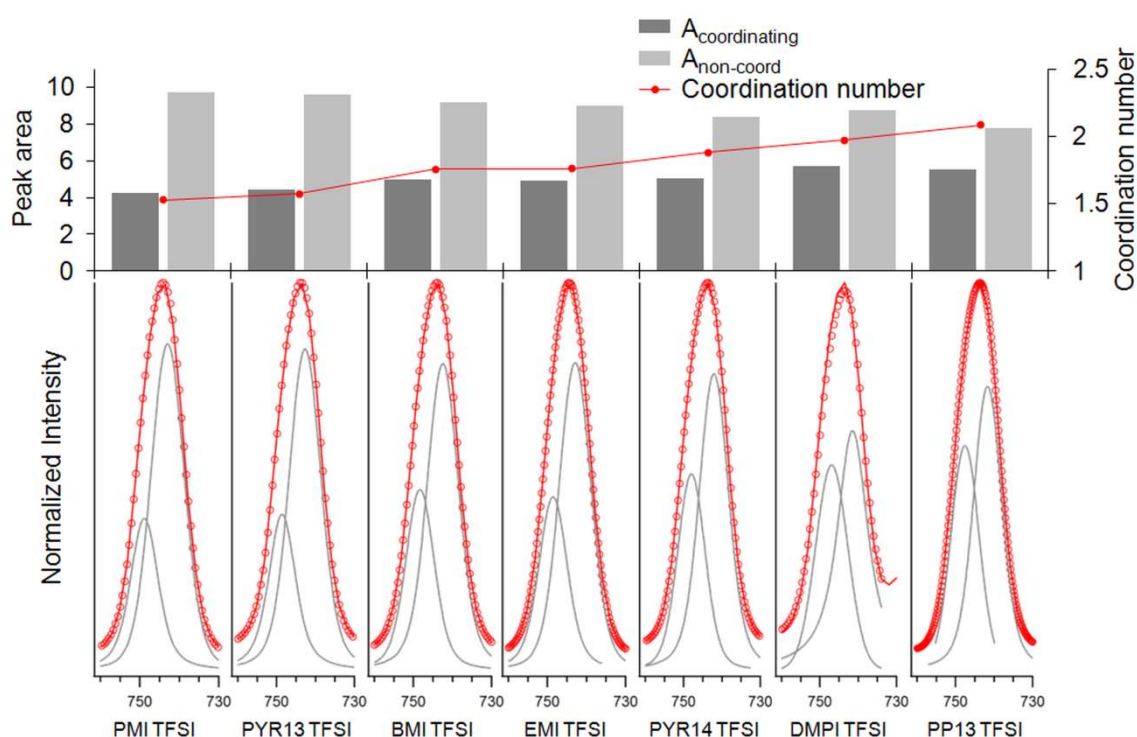


Figure 4. Raman spectra of solutions containing LiTFSI (molar fraction 0.2) and RTILs in the range between 760 and 730  $\text{cm}^{-1}$ . The red lines represent the measured data, the circles represent the fitted curve and the grey lines represent the two individual fitted peaks for coordinated and non-coordinated [TFSI]<sup>−</sup> anions.

Table 1. Composition, degradation temperature, H<sub>2</sub>O content, ionic conductivity, potential window and Li coordination number of the studied electrolytes.

Solvent / RTIL	Salt (x = 0.2)	Degradation temperature (°C)		H <sub>2</sub> O content (ppm)		Ionic conductivity at 25°C (mS cm <sup>−1</sup> )	Viscosity at 25°C (cP)	Potential window (V vs. Li <sup>+</sup> /Li)	Lithium coordination number
		Under N <sub>2</sub>	Under O <sub>2</sub>	Before drying	After drying				
TEGDME	Li TFSI	118	115	851	156	1.79	14.2	[0.1 ; 4.9]	-
PMI TFSI	Li TFSI	411	406	1062	33.1	2.3	102	[1.1 ; 5.4]	1.53
EMI TFSI	Li TFSI	407	369	3800	46	3.22	85.2	[1.3 ; 5.4]	1.76
EC:DEC (2:1vol)	Li PF <sub>6</sub>	88	75	22	-	8.87	5.1	[0.0 ; 5.7]	-
BMI TFSI	Li TFSI	405	362	110	43	1.42	102	[1.3 ; 6.2]	1.76
DMPI TFSI	Li TFSI	480	448	249	204	0.54	140	[1.1 ; 6.0]	1.97
PYR14 TFSI	Li TFSI	421	380	92	54	0.39	165	[0.2 ; 6.8]	1.88
PP13 TFSI	Li TFSI	406	413	2108	126	0.4	463	[0.1 ; 6.9]	2.08
PYR13 TFSI	Li TFSI	414	407	2031	78	0.8	206	[0.3 ; 6.6]	1.57

### Electrochemical characterization

The different electrolytes are further investigated in aprotic Li-O<sub>2</sub> batteries (Figure 5-A), for which the full discharge capacity is measured. The EC/DEC(2:1)-LiPF<sub>6</sub>, typically used for Li-ion batteries, presents a reasonable capacity of 775 mAh g<sup>-1</sup>. Concerning the RTILs with lithium salt, PP13 TFSI-LiTFSI, PYR13 TFSI-LiTFSI, PYR14 TFSI-LiTFSI and DMPI TFSI-LiTFSI have a specific capacity below 200 mAh g<sup>-1</sup>. This may be due to their high viscosity, leading to poor kinetics of the battery reaction.<sup>38</sup> These electrolytes have actually the lowest ionic conductivity, which indicates that a minimum is required for the Li-O<sub>2</sub> battery to work. However, this parameter is not directly correlated to the capacity neither the cyclability of the battery.<sup>39</sup> The TEGDME-LiTFSI shows clearly a higher capacity (4268 mAh g<sup>-1</sup>) than other electrolytes but not the highest ionic conductivity (1.79 mS cm<sup>-1</sup>). On the other hand, the viscosity of the electrolyte seems to be correlated to the capacity as the TEGDME-LiTFSI (14.2 cP) has a much lower value than the RTILs (> 85 cP). Concerning the PMI TFSI, EMI TFSI and BMI TFSI, they present a specific capacity of 559, 1408 and 1856 mAh/g respectively. Although the EMI TFSI has the lowest viscosity (85.2 cP), it seems that the lower lithium coordination number of the PMI TFSI (1.53 vs. 1.76 for the EMI TFSI) compensates the unfavorable transport properties of this RTIL. The BMI TFSI having both high viscosity and high lithium coordination number, the specific capacity is lower. Taking into account these results, the viscosity and the lithium solvation number are two determinant parameters influencing the mobility of the lithium cation and then the performance of the Li-O<sub>2</sub> battery.

The five electrolytes with the highest full capacity, i.e. TEGDME-LiTFSI, PMI TFSI-LiTFSI, EMI TFSI-LiTFSI, EC/DEC-LiPF<sub>6</sub> and BMI TFSI-LiTFSI are then tested in Li-O<sub>2</sub> cells cycled with controlled depth of discharge of 500 mAh g<sup>-1</sup>. The discharge and charge curves are shown in the Figure 5-B. Among these electrolytes, the TEGDME-LiTFSI has the best cyclability with 40 cycles. On the other hand, the EC/DEC-LiPF<sub>6</sub> shows no rechargeability. As it has been shown previously,<sup>40,41</sup> the carbonate electrolytes are not stable to nucleophilic attack by the superoxide radical (O<sub>2</sub><sup>-</sup>). Concerning the RTIL electrolytes, only 15 and 16 cycles are observed for the PMI TFSI-LiTFSI and EMI TFSI-LiTFSI respectively. The degradation of the electrolyte, observed during the electrochemical window measurement (Figure 6), may contribute to the consumption of solution components and the fast clogging of the cathode.

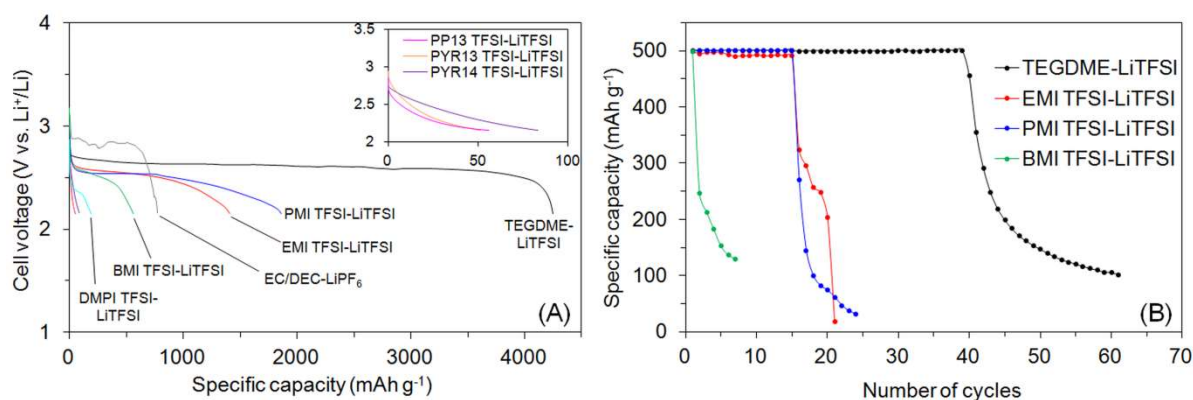


Figure 5. A) Initial discharge curve of Li-O<sub>2</sub> cells assembled with the different electrolytes studied, at a current of 100  $\mu$ A cm<sup>-2</sup>. B) Galvanostatic cycling test of Li-O<sub>2</sub> cells at a constant current of 75  $\mu$ A cm<sup>-2</sup>.

Indeed, observing the voltammetry curves shown in the Figure 6, all the imidazolium-based solutions, i.e. EMI TFSI-LiTFSI, PMI TFSI-LiTFSI, BMI TFSI-LiTFSI and DMPI TFSI-LiTFSI, present a reduction peak at 1.1 – 1.3 V vs. Li<sup>+</sup>/Li. This peak, that may be related to the deprotonation of the cation,<sup>42,43</sup> corresponds to the cathodic stability of the imidazolium RTILs. As this reaction occurs before the lithium plating (i.e. at 0 V vs. Li<sup>+</sup>/Li), there is degradation of the electrolyte during the cycling of the battery, explaining its low cyclability. The RTILs with non-aromatic cation such as PYR13 TFSI, PYR14 TFSI and PP13 TFSI, present a wider electrochemical stability window. The large reductive current observed around 0 V vs. Li<sup>+</sup>/Li corresponds to the reductive deposition of lithium onto the electrode. At the anodic potentials, the RTILs with lowest limit are EMI TFSI and PMI TFSI with 5.4 V vs. Li<sup>+</sup>/Li, which can be attributed to the oxidative decomposition of the TFSI<sup>-</sup> anion. For both organic solvent electrolytes, the anodic currents starting at 4.9 V vs. Li<sup>+</sup>/Li for the TEGDME and 5.7 V vs. Li<sup>+</sup>/Li for EC/DEC can be attributed to the oxidative decomposition of the electrolyte. In conclusion, RTILs have wide potential window, up to 6.6 V in the case of PYR14 TFSI-LiTFSI. Their electrochemical stability is directly related with the oxidation and reduction potential

values of the anions and cations respectively. That is why the medium is stable in the 2.15 – 4.35 V vs. Li<sup>+</sup>/Li operating voltage window of the battery for all the electrolytes except for those containing imidazolium RTILs.

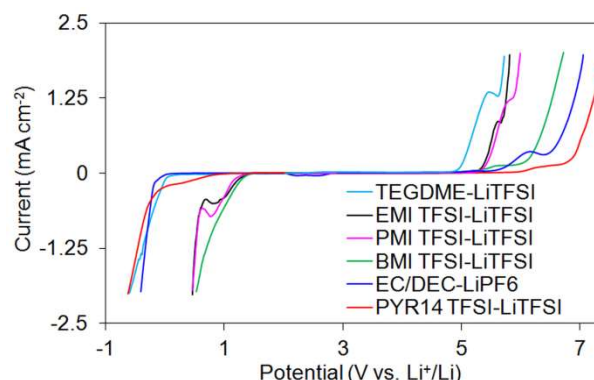


Figure 6. Linear sweep voltammograms of ionic liquids and organic electrolytes measured under argon atmosphere at 25 °C.

To summarize, the selection of an adequate electrolyte for Li-O<sub>2</sub> battery depends especially to the viscosity and the lithium coordination number of the solution. The viscosity has a direct influence on the kinetics of the battery reaction whereas the solvation of the lithium cation in the electrolyte may have an effect on the thermodynamics. As represented in the Figure 7, the highest capacities are situated at the low viscosity values. Then, for the electrolytes for which the viscosities are in the same range, a low lithium coordination number indicates a higher capacity. Nonetheless, the electrolyte has to be stable in the battery operating voltages, which is why the electrochemical stability window is a determinant parameter too.

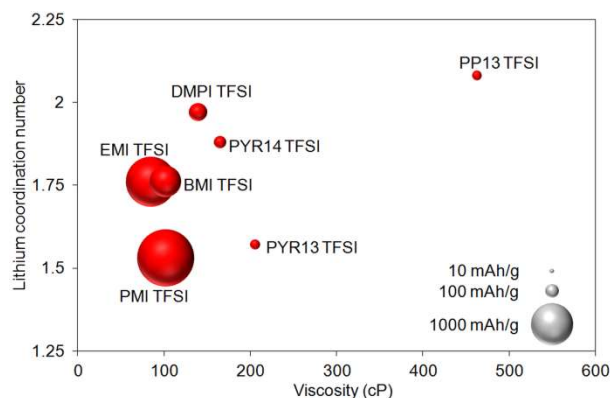


Figure 7. Representation of the specific capacity in function of the viscosity and lithium coordination number of the RTIL electrolyte.

## Conclusions

The properties of different electrolytes based on organic solvents and RTILs have been studied and tested in Li-O<sub>2</sub> batteries. The main advantage of ionic liquids over organic solvents is their high thermal stability, with a degradation temperature up to 480 °C in N<sub>2</sub>, whereas organic solvents evaporate completely above 150 °C. The ionic conductivity is increasing constantly within the temperature, reaching almost 8 mS cm<sup>-1</sup> for the EMI TFSI at 70 °C, which gives an interesting potential for application at medium and high temperature.<sup>44–46</sup> At room temperature, most of ionic liquids are in the same range than organic solvents with 3.33 mS cm<sup>-1</sup> for the EMI TFSI-LiTFSI. This value is equivalent to that of the TEGDME-LiTFSI, which is widely used for Li-O<sub>2</sub> batteries. The ionic liquids with an ionic conductivity below 1 mS/cm show very low specific capacity, below 200 mAh g<sup>-1</sup>. There is then a minimum needed but other parameters such as the viscosity and the lithium solvation number are more critical for the battery capacity. Indeed, the highest specific capacity is obtained with the TEGDME-LiTFSI (1.79 mS cm<sup>-1</sup>) with 4268 mAh per gram of carbon from the cathode for a full discharge. Imidazolium RTILs (EMI, PMI, BMI and DMPI) show capacities up to 1659 mAh g<sup>-1</sup>, higher than pyrrolidinium and piperidinium, which is attributed to a lower viscosity. However, the degradation of the imidazolium cation leads to low cyclability of the Li-O<sub>2</sub> cell.

## Acknowledgments

The STABLE project has received funding from the European Union's FP7 research and innovation program under grant agreement N° 314508. The authors thank Mr. Jerónimo Juan Juan from the University of Alicante (Spain) for the Raman measurements. G. G. thanks financial support from project CTQ2015-65439-R from the MINECO.

## References

- 1 K. M. Abraham and Z. Jiang, *J. Electrochem. Soc.*, 1996, **143**, 1–5.
- 2 P. G. Bruce, S. A. Freunberger, L. J. Hardwick and J.-M. Tarascon, *Nat. Mater.*, 2012, **11**, 19–29.
- 3 J. Christensen, P. Albertus, R. S. Sanchez-Carrera, T. Lohmann, B. Kozinsky, R. Liedtke, J. Ahmed and A. Kojic, *J. Electrochem. Soc.*, 2012, **159**, R1.
- 4 G. Girishkumar, B. D. McCloskey, A. C. Luntz, S. Swanson and W. Wilcke, *J. Phys. Chem. Lett.*, 2010, **1**, 2193–2203.
- 5 R. Padbury and X. Zhang, *J. Power Sources*, 2011, **196**, 4436–4444.
- 6 E. Commission and C. Action, [https://ec.europa.eu/clima/policies/international/negotiations/paris\\_en](https://ec.europa.eu/clima/policies/international/negotiations/paris_en) (accessed 2017-04-04), 2015, Climate Action.
- 7 J.-L. Shui, J. S. Okasinski, P. Kenesei, H. a Dobbs, D. Zhao, J. D. Almer and D.-J. Liu, *Nat. Commun.*, 2013, **4**, 2255.
- 8 J. Hou, M. Yang, M. W. Ellis, R. B. Moore and B. Yi, *Phys. Chem. Chem. Phys.*, 2012, **14**, 13487–13501.
- 9 S. Das, J. Højberg, K. B. Knudsen, R. Younesi, P. Johansson, P. Norby and T. Vegge, *J. Phys. Chem. C*, 2015, **119**, 18084–18090.
- 10 D. Sharon, D. Hirshberg, M. Afri, A. Garsuch, A. A. Frimer and D. Aurbach, *Isr. J. Chem.*, 2015, **55**, 508–520.
- 11 H. Nakamoto, Y. Suzuki, T. Shiotsuki, F. Mizuno, S. Higashi, K. Takechi, T. Asaoka, H. Nishikoori and H. Iba, *J. Power Sources*, 2013, **243**, 19–23.
- 12 J. Zeng, J. R. Nair, C. Francia, S. Bodoardo and N. Penazzi, *Int. J. Electrochem. Sci.*, 2013, **8**, 3912–3927.
- 13 C. O. Laoire, S. Mukerjee, K. M. Abraham, E. J. Plichta and M. A. Hendrickson, *J. Phys. Chem. C*, 2010, **114**, 9178–9186.
- 14 A. C. Luntz and B. D. McCloskey, *Chem. Rev.*, 2014, **114**, 11721–11750.
- 15 P. Bonhôte, A. Dias, N. Papageorgiou, K. Kalyanasundaram and M. Grätzel, *Inorg. Chem.*, 1996, **35**, 1168–1178.
- 16 M. C. Buzzeo, O. V. Klymenko, J. D. Wadhwani, C. Hardacre, K. R. Seddon and R. G. Compton, *J. Phys. Chem. A*, 2003, **107**, 8872–8878.
- 17 G. B. Appetecchi, M. Montanino, A. Balducci, S. F. Lux, M. Winterb and S. Passerini, *J. Power Sources*, 2009, **192**, 599–605.
- 18 C. J. Allen, J. Hwang, R. Kautz, S. Mukerjee, E. J. Plichta, M. a. Hendrickson and K. M. Abraham, *J. Phys. Chem. C*, 2012, **116**, 20755–20764.
- 19 D. Bresser, E. Paillard and S. Passerini, *J. Electrochem. Sci. Technol.*, 2014, **5**, 37–44.
- 20 S. Ferrari, E. Quartarone, C. Tomasi, M. Bini, P. Galinetto, M. Fagnoni and P. Mustarelli, *J. Electrochem. Soc.*, 2014, **162**, A3001–A3006.
- 21 S.-M. Han, J.-H. Kim and D.-W. Kim, *J. Electrochem. Soc.*, 2015, **162**, A3103–A3109.
- 22 J. Kim, E. Ahn and Y. Tak, *Int. J. Electrochem. Sci.*, 2015, **10**, 2921–2930.
- 23 K. Cai, H. Jiang and W. Pu, *Int. J. Electrochem. Sci.*, 2014, **9**, 390–397.
- 24 L. Cecchetto, M. Salomon, B. Scrosati and F. Croce, *J. Power Sources*, 2012, **213**, 233–238.
- 25 J.-C. Lassègues, J. Grondin, C. Aupetit and P. Johansson, *J. Phys. Chem. A*, 2009, **113**, 305–314.
- 26 T. Brousse, P.-L. Taberna, O. Crosnier, R. Dugas, P. Guillemet, Y. Scudeller, Y. Zhou, F. Favier, D. Bélanger and P. Simon, *J. Power Sources*, 2007, **173**, 633–641.
- 27 J. Zeng, J. R. Nair, C. Francia, S. Bodoardo and N. Penazzi, *Solid State Ionics*, 2014, **262**, 160–164.
- 28 D. J. Lee, J. Hassoun, S. Panero, Y. K. Sun and B. Scrosati, *Electrochem. commun.*, 2012, **14**, 43–46.
- 29 D.-J. Lee, J.-W. Park, I. Hasa, Y.-K. Sun, B. Scrosati and J. Hassoun, *J. Mater. Chem. A*, 2013, **1**, 5256.

- 30 J. H. Shin and E. J. Cairns, *J. Electrochem. Soc.*, 2008, **155**, A368.
- 31 B. Garcia, S. Lavallée, G. Perron, C. Michot and M. Armand, *Electrochim. Acta*, 2004, **49**, 4583–4588.
- 32 T. J. Wooster, K. M. Johanson, K. J. Fraser, D. R. MacFarlane and J. L. Scott, *Green Chem.*, 2006, **8**, 691.
- 33 D. Capsoni, M. Bini, S. Ferrari, E. Quartarone and P. Mustarelli, *J. Power Sources*, 2012, **220**, 253–263.
- 34 Y. Litaïem and M. Dhahbi, *J. Mol. Liq.*, 2012, **169**, 54–62.
- 35 T. Vogl, P. Goodrich, J. Jacquemin, S. Passerini and A. Balducci, *J. Phys. Chem. C*, 2016, **120**, 8525–8533.
- 36 S. Menne, T. Vogl and A. Balducci, *Phys. Chem. Chem. Phys.*, 2014, **16**, 5485.
- 37 M. Kerner, N. Plylahan, J. Scheers and P. Johansson, *Phys. Chem. Chem. Phys.*, 2015, **17**, 19569–19581.
- 38 C. O. Laoire, S. Mukerjee, K. M. Abraham, E. J. Plichta and M. a. Hendrickson, *J. Phys. Chem. C*, 2009, **113**, 20127–20134.
- 39 G. A. Giffin, A. Moretti, S. Jeong and S. Passerini, *J. Power Sources*, 2017, **342**, 335–341.
- 40 F. Mizuno, S. Nakanishi, Y. Kotani, S. Yokoishi and H. Iba, *Electrochem. commun.*, 2010, **78**, 403–405.
- 41 B. D. McCloskey, D. S. Bethune, R. M. Shelby, G. Girishkumar and A. C. Luntz, *J. Phys. Chem. Lett.*, 2011, **2**, 1161–1166.
- 42 J. Dupont and P. A. Suarez, *Phys. Chem. Chem. Phys.*, 2006, **8**, 2441–2452.
- 43 P. A. Z. Suarez, C. S. Consorti, R. F. De Souza, J. Dupont and R. S. Gonçalves, *J. Braz. Chem. Soc.*, 2002, **13**, 106–109.
- 44 R. Lin, P.-L. Taberna, S. Fantini, V. Presser, C. R. Pérez, F. Malbosc, N. L. Rupasinghe, K. B. K. Teo, Y. Gogotsi and P. Simon, *J. Phys. Chem. Lett.*, 2011, **2**, 2396–2401.
- 45 N. Plylahan, M. Kerner, D. H. Lim, A. Matic and P. Johansson, *Electrochim. Acta*, 2016, **216**, 24–34.
- 46 A. Balducci, R. Dugas, P. L. Taberna, P. Simon, D. Plée, M. Mastragostino and S. Passerini, *J. Power Sources*, 2007, **165**, 922–927.